RSC Advances

PAPER

View Article Online
View Journal | View Issue

Cite this: *RSC Adv.*, 2017, **7**, 49937

Influence of defects induced by chemical treatment on the electrical and thermal conductivity of nanofluids containing carboxyl-functionalized multi-walled carbon nanotubes

Pham Van Trinh, *[a] Nguyen Ngoc Anh,[a] Nguyen Trong Tam,[b] Nguyen Tuan Hong,[c] Phan Ngoc Hong,[ab] Phan Ngoc Minh[abc] and Bui Hung Thang*[a]

In this paper, we present the results on the influence of chemical treatment time on the structure of carboxyl-functionalized MWCNTs (MWCNT–COOH) and their nanofluids. The morphological and structural studies investigated by FTIR, HRTEM and Raman scattering demonstrated that the structural defects of MWCNT–COOH increase with increasing chemical treatment time. Nanofluids containing MWCNT–COOH treated for a longer time showed better stability due to the increasing of COOH functional groups attached to the surface of MWCNTs. The electrical conductivity of the nanofluids increases with increasing CNT concentration and decreases with increasing chemical treatment time. The thermal conductivity of the nanofluids enhanced when increasing CNT concentration and reached the highest value for MWCNT–COOH with 5 h chemical treatment. By using the effective medium theory (EMT) and experimental data fitting, the thermal boundary resistance (TBR) and the thermal boundary conductance (TBC) of MWCNT–COOH/water were found to be 90 $\times$ 10^{-8} m^2 K W^{-1} and 1.1 MW m^{-2} K^{-1}, respectively. The interfacial layer thermal conductivity (K_i) between CNTs and base fluid was estimated by using Murshed's model. The highest K_i was obtained to be 2.6 W m^{-1} K^{-1} for a nanofluid with 5 h chemical treatment. The results implied that the thermal conductivity of CNT based nanofluids could be improved by increasing the K_i *via* optimizing of the chemical treatment conditions.

Received 2nd August 2017
Accepted 20th October 2017

DOI: 10.1039/c7ra08552d

rsc.li/rsc-advances

1. Introduction

Because of the unique properties demonstrated by both theoretical and experimental studies, carbon nanotubes (CNTs) have received great attention from researchers and manufacturers for many potential applications in industry fields.[1–3] Among these potential applications, using CNTs as heat transfer media in high thermal conductivity nanofluids for cooling systems is one of the most promising and interesting applications due to their high thermal conductivity, high electrical conductivity and low density.[4–11] The problem here is it is challenging to disperse CNTs in solvents directly for preparing nanofluids due to their high hydrophobicity in as-grown states and CNTs normally tend to aggregate together to form bundles or clusters due to van der Waals interactions. As presented in many reports, maintaining uniform dispersion and stability of CNT nanofluids is a key point to obtain the optimal thermal properties for a long time. This problem could be resolved by using two main methods including chemical and physical treatments.[5,12] In which, chemical treatments seem to be more effective due to provide a solution for nanoscale dispersion with increasing the interaction between the CNT and base fluid molecules *via* atomic bonding.[13] The chemical treatment is normally classified into non-covalent functionalization and covalent functionalization.[5,12,13] In basically, non-covalent functionalization does not influence the structure of CNTs by using several conventional surfactants such as gum arabic (GA), sodium deoxycholate (DOC), sodium dodecyl benzene sulfonate (SDBS), sodium dodecyl sulfate (SDS), hexadecyl trimethyl ammonium bromide (CTAB) and chitosan, *etc.* Many studies demonstrated that non-covalent functionalization could keep the stability of CNT nanofluids for a long time.[14–18] Contrary to non-covalent functionalization, covalent functionalization could modify the structure of CNTs due to the strong chemical reaction during the hydrophilic functional group attachment. This method extensively uses an aqueous solution of acids or oxidizing agents including nitric acid (HNO_3), sulfuric acid (H_2SO_4), hydrochloric acid (HCl) or hydrogen peroxide (H_2O_2) to covalently functionalize.[19–21] The method has exhibited an effective

[a]*Institute of Materials Science, Vietnam Academy of Science and Technology, 18 Hoang Quoc Viet Str., Cau Giay Distr., Hanoi, Vietnam. E-mail: trinhpv@ims.vast.vn; thangbh@ims.vast.ac.vn; Tel: +84 943190301*

[b]*Graduated University of Science and Technology, Vietnam Academy of Science and Technology, 18 Hoang Quoc Viet Str., Cau Giay Distr., Hanoi, Vietnam*

[c]*Center for High Technology Development, Vietnam Academy of Science and Technology, 18 Hoang Quoc Viet Str., Cau Giay Distr., Hanoi, Vietnam*

to obtain uniform dispersions and long-time stability of nanofluids due to eliminating the van der Waals forces among CNTs *via* hydrogen bonding between functional groups attached to the surface of CNTs and base fluids.[4,5] In addition, the presence of the functional groups such as COOH, OH and NH_2, … is beneficial for compacting with other nanoadditives including nanoparticle, nanosheets to make the hybrid nanomaterials for nanofluid applications.[22–24] Therefore, the covalent functionalization is more often used compared to non-covalent functionalization due to sufficient for maintaining the stability not only for CNT nanofluids but also for CNT hybrid nanofluids as mentioned.[25]

The properties of CNTs based nanofluids such as the thermal conductivity, heat transfer, electrical conductivity, viscosity, stability have been investigated and reported.[5,8–10,26–36] Many works have been proposed and mainly focused on the thermal property both in the experimental and the theoretical models due to high thermal conductivity of CNTs compared to other materials and high potential applications.[26–33] These works have almost been done to investigate the effect of the parameters such as CNT structure, CNT concentration, temperature, pH, surfactants, ultrasonic power, ultrasonication time on this property.[26–33] The role of surfactants is well-known for CNT dispersion but their contribution to the thermal conductivity of nanofluid are not very clearly.[5,26,31] Meibodi *et al.* reported that the surfactant weight percent of SDBS and GA is not a significant factor on the thermal conductivity of nanofluids.[26] In similar, Estellé *et al.* also demonstrated that the surfactant is beneficial for better dispersant but does not affect to the thermal conductivity of nanofluid.[31] In contrary to the thermal conductivity, just a few studies concerning to the electrical conductivity of CNT based nanofluids have been done and presented.[34–36] These studies have also been investigated the effect of the same parameters as done with the thermal conductivity. Glory *et al.* reported the electrical conductivities of CNT/water nanofluid as a function of temperature, nanotube weight content, and nanotube length.[34] Kumar *et al.* investigated the effect of the surfactant (GA) and temperature on the electrical conductivity of MWCNT based nanofluids.[35] Al-Sharafi *et al.* reported the depending upon the volumetric concentration of CNTs and their distribution on the electrical property of nanofluid.[36] According to literature, there are still no studies that have been done to investigate the effects on of the covalent functionalization method on the thermal conductivity enhancement of CNT based nanofluids up to now. How the defects introduced CNTs during treatment affect the properties of CNT based nanofluids still a big question that needs to be clarified.

Thus, in this paper, we present for the first time the effect of chemical treatment time of the covalent functionalization on the thermal and electrical conductivity of nanofluids containing carboxyl-functionalized multi-walled carbon nanotubes (MWCNTs). In addition to the experimental results, several theoretical models were used to validating the obtained data and estimating the unknown factors that effect to the thermal conductivity of nanofluid such as the thermal boundary resistance, the thermal boundary conductance and the interfacial layer thermal conductivity of CNTs and based fluids.

2. Experiment procedure

In this paper, lab-made MWCNTs were used with an average around 20 nm in diameter and 10 μm in length synthesized by a chemical vapor deposition (CVD) technique using $Fe/CaCO_3$ as catalytic material.[37] Sulphuric acid (H_2SO_4, 98%) and nitric acid (HNO_3, 68%) supplied by Xilong Chemical Co., Ltd (China) were used for functionalization process.

MWCNTs were functionalized with a carboxyl group (–COOH) by treatment in the mixture of acid (HNO_3 : H_2SO_4, 1 : 3) at 70 °C for a different treatment time of 3 h, 5 h and 7 h under continuous magnetic stirring. After chemical treatment process, the obtained solutions were filtered and cleaned by distilled water for several times until no residual acid was detected (pH ≈ 7). After cleaning, the samples were noted as C3, C5 and C7 corresponding to 3 h, 5 h and 7 h treatment times, respectively. A calculated amount of each C3, C5 and C7 were dispersed in distilled water to prepare nanofluids with a different MWCNT concentration of 0.16, 0.32, 0.48, 0.64 and 0.80 vol% by ultrasonication for 45 min under cool water. Nanofluids with higher CNT concentrations were not prepared and investigated to limit the effect of the CNT aggregation on the properties of nanofluids.

FTIR spectra of samples were recorded using a SHIMADZU IR Prestige21 Spectrometer. A high-resolution transmission electron microscopy (HRTEM, Jeon-JEM 2100) was used was used for microstructural characterization. Raman scattering measurements were carried out using an iHR550 Jobin-Yvon spectrometer with 514 nm laser excitation. A Malvern ZS Nano S Analyzer (London, UK) was used to check the aggregation size distribution and the stability of nanofluids. The electrical conductivity was measured by HI 993302-02 Monitor supplied by Hanna Instruments with an accuracy of ±2%. To evaluate exactly the effect of the chemical treatment time and reduce the Brown motion effect on the thermal conductivity of nanofluids, the thermal conductivity was measured at a fixed temperature of 30 °C using an HTL-04 equipment (Eternal Engineering Equipment Ltd., India). The equipment bases on principle of the guarded hot plate (GHP) method with a maximum uncertainty of ±2%. The measurements performed on the same conditions and experimental data were the average of 15 measurements.

3. Results and discussion

Fig. 1 shows the FTIR spectra of the functionalized MWCNTs with the different chemical treatment time of 3 h, 5 h and 7 h. Spectra show several important bands located at in all samples. The band at 3426 cm^{-1} is assigned to the vibration of the O–H bonding. The band of the C=C bonding of the CNT structure appears at 1580 cm^{-1}. The band at 1720 cm^{-1} is assigned to the vibration of the C=O bonding in the carboxyl (–COOH) group. This is an important characteristic to demonstrate the attachment of the carboxylic group (–COOH) on the surface of

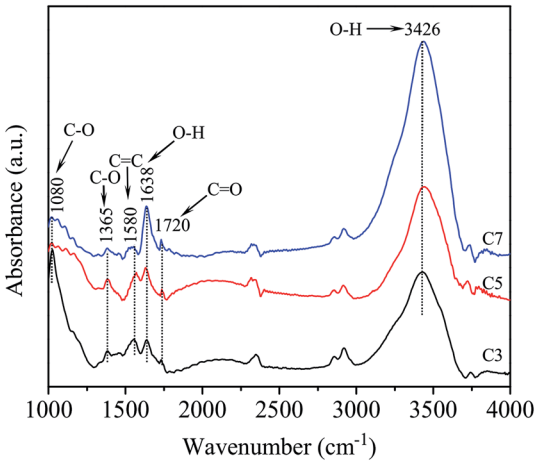

Fig. 1 FTIR spectrum of carboxyl-functionalized multi-walled carbon nanotubes.

MWCNTs.[38] FTIR spectra are also shown the band at 1080 cm^{-1}, which is a typical band of the C–O bonding in the COOH group.[39] In addition, it was found that as chemical treatment time increases, the intensity of the absorption bands of the C=O bond increase, possibly due to the increasing amount of COOH groups on the surface of CNTs. In contrary, the absorption intensity of the bands of C=C bonding decrease as the chemical treatment time increases. This could be due to increasing of the treatment time that has resulted in structural defects, C=C bonding in MWCNTs have been fractured by corrosion and addition of COOH functional groups. Basing on FTIR spectrum analysis above could confirm that the functionalization process of MWCNTs by chemical treatment a mixture of HNO_3 and H_2SO_4 acid helps to attach the COOH groups on the surface of the MWCNTs. The absorption intensity of the C=O bonding increases and the C=C bonding decreases when chemical treatment time increases due to the effects of structural defects caused by chemical etching and the existence of COOH groups.

Fig. 2 shows the HRTEM images of MWCNTs functionalized with different chemical treatment time. For as-grown MWCNTs, as can be seen, the structure is nearly perfect with no etched or defect points and a distance between walls was determined about 0.34 nm (Fig. 2a and b). While for functionalized MWCNTs, when the chemical treatment time increases, the concentration of structural defect points increases. For C3, structural defects start appearing at outside walls, several etched points are observed in Fig. 2c and d. These structural defects are attributed to the effect of chemical reagents during the COOH functionalized process. This has been reported and discussed in several reports.[40,41] As the chemical treatment time increased to 5 hours, besides defects observed at outside walls, some defects starting appeared on the inside walls of the MWCNTs as broken points (Fig. 2e and f). In the same research topic, Zhang *et al.* also identified the sidewall C–C broken bond caused by covalent functionalization.[42] When the treatment time increased up to 7 hours, besides of the defect points, the crystallite structure of MWCNTs becomes harder to identify as expressive as those of as-grown MWCNTs (Fig. 2g and h). Rebelo *et al.* reported that the covalent functionalization of MWCNT by oxidation methods will cause defects and leads to structure burning.[43] Thus, as results, we can conclude that the longer chemical treatment time will cause more defect points on the structure of MWCNTs.

Fig. 3 shows Raman spectra of MWCNT–COOH with different chemical treatment times. Two typical peaks at 1348.95 cm^{-1} and 1582.97 cm^{-1} are assigned to the defect band (D) and the graphitic band (G), respectively. The relative intensity ratio of D to G (I_D/I_G) of samples was determined to be 0.92, 0.93, 1.02 and 1.05 corresponding to as-grown MWCNTs, C3, C5, and C7, respectively. The I_D/I_G ratio of samples with more prolonged treatment time is higher and the intensity ratio I_D/I_G increase when the treatment time increases. This results proved that the chemical treatment time strongly affects to the CNT structure. The results of the Raman analysis are consistent with the results of the HRTEM study presented earlier.

The effect of chemical treatment time on aggregate size distribution and zeta potential of the nanofluid C3, C5 and C7 with the same CNT concentration of 0.8 vol% is shown in Fig. 4. As can be seen in Fig. 4a, the peak of aggregate size for nanofluids reduced when increasing the chemical treatment time from 3 h to 7 h. The average of aggregated size was measured about 295 nm, 540 nm and 885 nm corresponding to nanofluid C3, C5 and C7, respectively. It means that the most significant aggregate size was observed for MWCNTs with 3 h chemical treatment time and the smallest aggregate size was observed for MWCNTs functionalized in 7 h. This could be due to both the effect of strong acid reagents on the decrease of MWCNT length during a chemical reaction and the increase in the number of COOH groups on the surface of MWCNTs that helped to uniformly disperse the functionalized MWCNTs *via* a hydrogen bonding between COOH groups and water. The shortening and separating of MWCNT by chemical treatment help to uniformly dispersed MWCNTs into the base fluids and resulting in the higher stability of nanofluids.[44]

Zeta potential was used for estimating the stability of the nanofluid C3, C5 and C7. As shown in Fig. 4b, the average potential values were measured to be −15.6 mV, −37.7 mV and −48.03 mV corresponding to nanofluid C3, C5 and C7, respectively. It is well-known that zeta potential is the difference in the potential between the base fluids and the stationary layer that attached to the nanoparticles and its values could represent to the stability of nanofluids. The absolute zeta potential values for the stability region of colloids in fluids were defined as follows: 0–15 mV as little or no stability, 15–30 mV as some stability but settling lightly, 30–45 moderate stability, 45–60 mV as good and over 60 as excellent.[45,46] In general, a nanofluid with an absolute zeta-potential value above 30 mV is considered to have good stability.[45] So, the nanofluids contained the functionalized MWCNTs with chemical treatment times longer than 5 h show a better stability compared to that of 3 h chemical treatment. It is attributed to the increase the COOH groups attached on the surface of MWCNTs when increasing the chemical treatment time led to improving the dispersion and the stability of nanofluids.

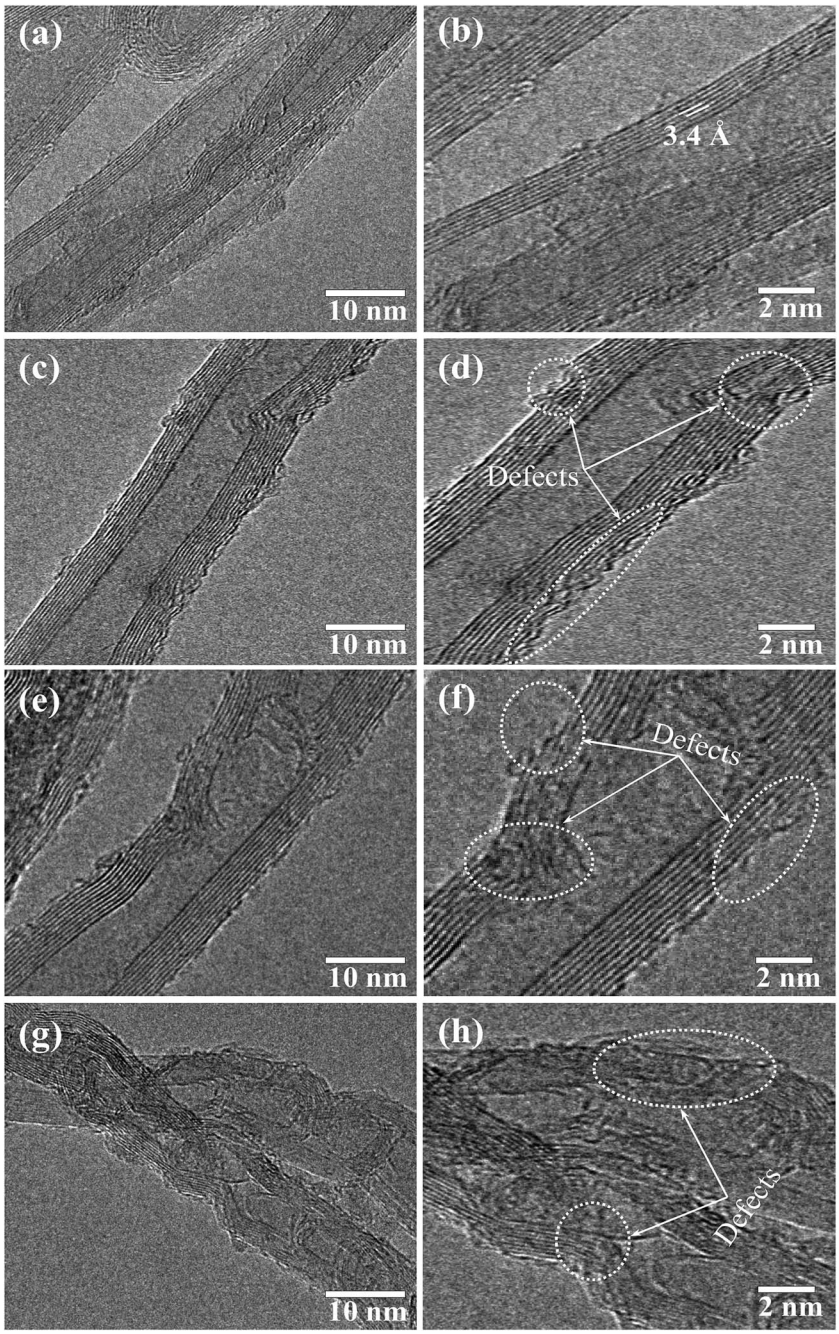

Fig. 2 HRTEM images of (a and b) CNTs, (c and d) sample C3, (e and f) sample C5 and (g and h) sample C7.

Fig. 5 shows the electrical conductivity of the nanofluid C3, C5 and C7. It can be seen that the electrical conductivity increases with increasing CNT concentrations. This was attributed to the decrease of the free path that allows enhancing the free carrier transports between the MWCNTs. The dependence of the electrical conductivity on the CNT concentration is more clear in nanofluids that contained functionalized MWCNTs with shorter treatment time and become nearly not significant when the treatment time is longer. The electrical conductivity of nanofluids decreases with the increase of chemical treatment times. This could be due to increasing the number of COOH group concentration, the defects on the surface of MWNTs and the cutting of MWCNTs. As results, it is interesting to note that the nanofluid C3 even reveals a higher agglomerated size distribution and a lower stability, still shows a higher electrical conductivity compared to other nanofluids. It means the uniform dispersion of MWCNTs seems not to be a critical reason that affects to the increase of the electrical conductivity of nanofluids compared to the structural defects caused by chemical functionalization process. The higher electrical conductivity of the nanofluids with the agglomerated state compared to the uniformly dispersed state possible related to

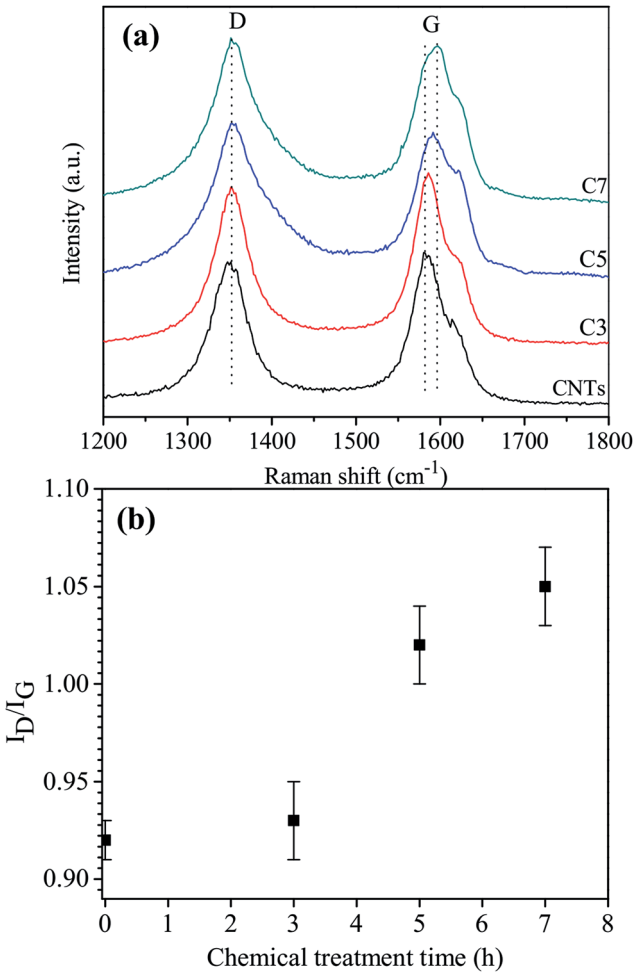

Fig. 3 (a) Raman spectra and (b) I_D/I_G ratio of carboxyl-functionalized multi-walled carbon nanotubes.

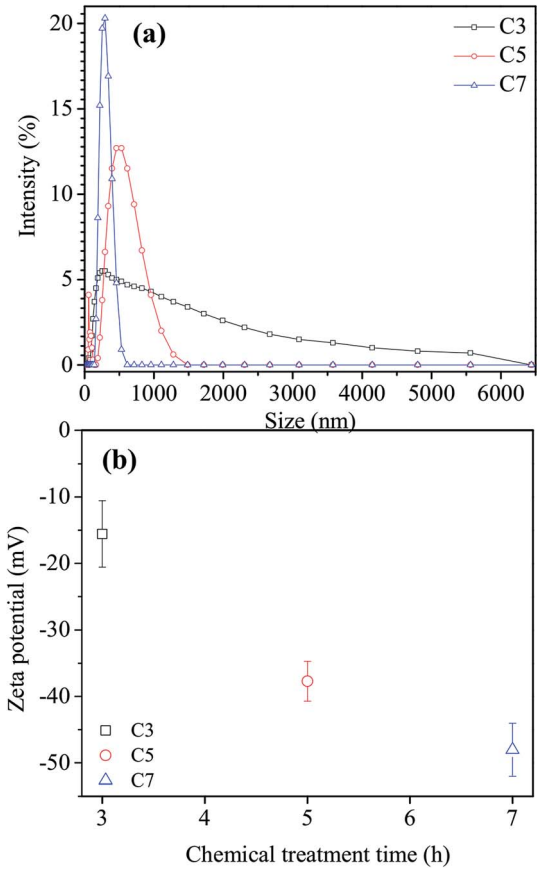

Fig. 4 (a) Size distribution and (b) zeta potential of the nanofluid C3, C5 and C7 with the same CNT concentration of 0.8 vol%.

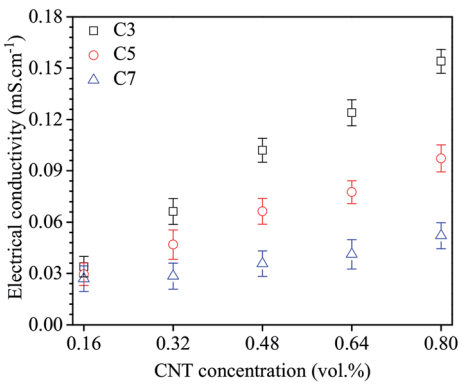

Fig. 5 Electrical conductivity of nanofluids *versus* CNT concentrations.

the increase of CNT-to-CNT contact/junctions in the percolating network formed by the CNT aggregations that allowed for electron tunneling and moving inside.[47] This distance has been reported in a range from 5 to 30 nm.[48] However, it is noted that the conductivity may not significantly improve if CNT-to-CNT distance is larger than the limit of the electron tunable distance.

The thermal conductivity of the nanofluid C3, C5 and C7 was investigated. Before conducting the thermal conductivity measurements, the thermal conductivity of distilled water was measured at a temperature of 30 °C to validate and calibrate the measurement technique. The measured thermal conductivity of 0.606 W m^{-1} K^{-1} and compared to the reference value of 0.607 W m^{-1} K^{-1}.[49] The measured value is in good agreement with the reference value and the uncertainty of the thermal conductivity measurement is within ±2%. Fig. 6 shows the thermal conductivity of nanofluids as a function of MWCNT concentration measured at 30 °C. As seen in all nanofluids, the thermal conductivity of nanofluids increases with increasing of MWCNT concentration. The relationship between MWCNT concentration and the thermal conductivity was reported in many studies.[50–53] Almost these reports have confirmed that the increase of thermal conductivity of nanofluids with increasing CNT loading is mainly due to the decrease of the distance or mean free path *via* a percolation effect resulted from increasing the frequency of lattice vibration.[39]

The influence of chemical treatment time of MWCNT on the thermal conductivity of nanofluids is also observed. Unlike with the electrical conductivity, the thermal conductivity reaches to highest value for nanofluid C5 and then decrease immediately for

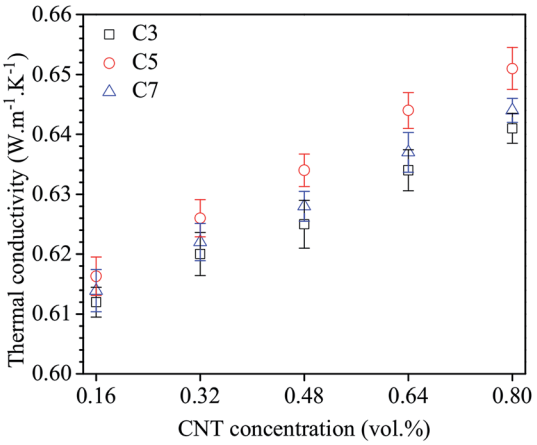

Fig. 6 Thermal conductivity of nanofluids *versus* CNT concentrations measured at 30 °C.

nanofluid C7. According to Munkhbayar *et al.*, three factors including (i) straightness ratio, (ii) specific surface area and (iii) CNT aggregation may keep significant roles in the thermal conductivity enhancement of CNT based nanofluids.[54] For the first factor, Xie and Chen also reported that the heat transports inside CNTs as well as at interface regions between CNTs and base fluid become more effective if the straightness ratio increases and resulting in the thermal conductivity enhancement.[55] For the second factor, many studies have been done to explain the mechanism of thermal conductivity enhancement in a nanofluid by specific surface area in the literature.[4,54–56] According to these reports, when increasing the specific surface area of nano-additives will lead to improving the thermal conductivity of nanofluid as resulted from the increase of the interaction and collision among nanoadditives. For the third factor, the effect of the CNT aggregations on thermal conductivity of nanofluids have been presented and discussed in many reports.[55,57] Most of the studies agreed that the thermal conductivity could be improved by decreasing the aggregation of MWCNTs. This is because the nanofluids containing individual CNTs are believed to have a quicker heat transports compared to the nanofluids containing aggregated and/or bundled CNTs. From above comments, it is evident that the improvement of thermal conductivity of nanofluid C5 compared to nanofluid C3 is mainly due to the difference in the aggregation state of the nanofluids. Nanofluid C5 showed a better dispersion and stability and thus higher thermal conductivity. However, when increasing the chemical treatment time from 5 h (C5) to 7 h (C7), the thermal conductivity of nanofluid decrease immediately. Interestingly here is why nanofluid C7 exhibited the dispersion and stability much better, still has a lower thermal conductivity than those of nanofluid C5. This is very difficult to explain by using the factors such as straightness ratio, specific surface area and CNT aggregation. In this case, the decrease of the thermal conductivity may be due to the destruction of the graphitic structure of MWCNTs by strong chemical reagents for a longer time as discussed earlier in morphological and microstructural studies. It is well-known, by using molecular dynamics (MD) simulations, many authors demonstrated that the thermal conductivity decreases significantly even at low defect concentrations.[48] So, the conclusion can be drawn from the results that the increasing chemical treatment time could improve the dispersion stability and the thermal conductivity of nanofluids however the thermal conductivity will significantly decrease if treatment time is too long.

To evaluate the effect of chemical treatment time to the interfacial thermal transport between the MWCNTs and based fluid, Maxwell-Garnett type Effective Medium Theory (EMT) model proposed by Nan *et al.*[17,18,58] have been used along with the TBR fitting. The model not only takes into account many factors such as shape, size, aspect ratio, orientation, CNT concentration but also includes the anisotropic thermal transport and the interfacial thermal transport. The thermal conductivity ratio of nanofluids according to Nan's model was estimated using the following equation:

$$\frac{K_{nf}}{K_{bf}} = 1 + \frac{\phi L_{CNT}}{d_{CNT}} \frac{K_{CNT}/K_{bf}}{(L_{CNT}/d_{CNT}) + (2a_k/d_{CNT})(K_{CNT}/K_{bf})} \quad (1)$$

here

$$a_k = \mathrm{TBR} \times K_{CNT} \quad (2)$$

where, K_{nf}, K_{CNT} ($\approx$1800 W m^{-1} K^{-1})[59] and K_{bf} ($\approx$0.6 W m^{-1} K^{-1}) are the thermal conductivity of the nanofluid, MWCNTs and the base fluid, respectively. ϕ, L_{CNT} ($\approx$10 μm) and d_{CNT} ($\approx$20 nm) are the concentration, length and diameter of MWCNTs. TBR is the thermal boundary resistance between the MWCNT and base fluid.

Fig. 7 shows the comparison of experimental results for nanofluid C3, C5 and C7 with the calculated data of the EMT incorporated the TBR. By using the EMT fitting, the TBR could be estimated to be 120 × 10^{-8} m^2 K W^{-1}, 90 × 10^{-8} m^2 K W^{-1} and 110 × 10^{-8} m^2 K W^{-1} and the TBC (inverse of TBR) of 0.8 MW m^{-2} K^{-1}, 1.1 MW m^{-2} K^{-1} and 0.91 MW m^{-2} K^{-1} corresponding to nanofluid C3, C5 and C7, respectively. As results, the TBC of nanofluid C5 is the highest value compared to others, again confirmed that the best chemical treatment time is to be 5 h. This treatment time does not only keep the stability

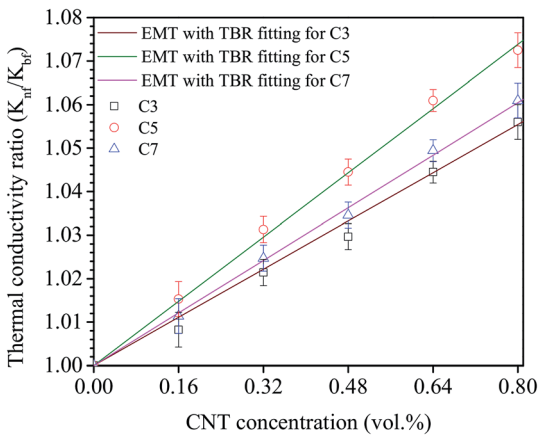

Fig. 7 Comparison of experimental results with the effective medium theory incorporated the thermal boundary resistances.

for a long time but also improve the thermal conductivity of nanofluids by enhancing the TBC between MWCNTs and base fluid. The decrease of TBC of nanofluid C3 could be due to the chemical treatment time of 3 h quite short that not enough time to attach the required COOH groups on the surface of MWCNTs and thus the bonding between MWCNTs and base fluid become more weakly compared to the nanofluid C5. The weak bonding could cause the stronger phonon scattering at the interface and thus lead to decrease the TBC. In addition, the aggregation of MWCNTs in nanofluid C3 caused by the weak bonding as discussed in the stability section will lead to forming a new boundary between MWCNT and MWCNT. This boundary always contributes a new TBR of CNT–CNT boundary. So, the contribution of TBR of MWCNT and base fluid along with TBR of MWCNT–MWCNT boundary is a factor leading to increase the TBR or decrease the TBC of nanofluid C3. In contrary, the decrease of TBC in nanofluid C7 not because of either the weak bonding or the aggregation of MWCNT. This is attributed to the chemical treatment time is too long led to increasing the defects and disorders in the graphite structure of MWCNT not only outside walls but also inside walls. These defects will restrict the phonon transports by scattering lead to the reduction of the phonon mean free path. Fthenakis *et al.* also reported that the reduction of the phonon mean free path is the main reason for the decrease of the thermal conductivity in defective systems.[60] Chiavazzo *et al.* presented the results of using a molecular dynamics (MD) simulation calculate of TBC of SWCNT/water and found the TBC value about 10 MW m^{-2} K^{-1}.[61] Similarly, Hida *et al.* also reported the TBC of CNT/polyethylene at room temperature to be 10 MW m^{-2} K^{-1}.[62] In the experiment, Harish *et al.* reported the value of TBC of SWCNT/water with DOC used as the surfactant to be 300 MW m^{-2} K^{-1} and 145 MW m^{-2} K^{-1} as using EMT and Yamada–Ota with TBR fitting, respectively.[17,18] Huxtable *et al.* and Carlborg *et al.* reported that carbon nanotube based nanofluids have a lower TBC in the range of 2.4–12 MW m^{-2} K^{-1}.[63,64] The obtained TBC values in this study are quite low compared to these reported values. This could be attributed to the following reason: (i) almost reported results were calculated for SWCNT with very high thermal conductivity by simulations with defect-free; (ii) the presence of the structural defects caused by chemical treatment may reduce the TBC as resulted from the phonon scattering in all directions of the MWCNTs.

Besides, several theoretical models such as Maxwell model, Hamilton–Crosser (H–C) model, Thang's model, Patel's model and Xue's model were also used to estimate the effective thermal conductivity (K_{nf}/K_{bf}) of the nanofluids as follows:

Maxwell's model[65]

$$\frac{K_{nf}}{K_{bf}} = \frac{K_{CNT} + 2K_{bf} + 2\phi(K_{CNT} - K_{bf})}{K_{CNT} + 2K_{bf} - \phi(K_{CNT} - K_{bf})} \quad (3)$$

H–C model[66]

$$\frac{K_{nf}}{K_{bf}} = \frac{K_{CNT} + (n-1)K_{bf} - (n-1)\phi(K_{bf} - K_{CNT})}{K_{CNT} + (n-1)K_{bf} + \phi(K_{bf} - K_{CNT})} \quad (4)$$

Thang's model[67]

$$\frac{K_{nf}}{K_{bf}} = 1 + \frac{1}{3}\frac{K_{CNT}\phi r_{bf}}{K_{bf}(1-\phi)r_{CNT}} \quad (5)$$

Patel's model[68]

$$\frac{K_{nf}}{K_{bf}} = 1 + \frac{K_{CNT}\phi r_{bf}}{K_{bf}(1-\phi)r_{CNT}} \quad (6)$$

Xue's model[69]

$$\frac{K_{nf}}{K_{bf}} = \frac{1-\phi+2\phi((K_{CNT})/(K_{CNT}-K_{bf}))\ln((K_{CNT}+K_{bf})/2K_{bf})}{1-\phi+2\phi((K_{bf})/(K_{CNT}-K_{bf}))\ln((K_{CNT}+K_{bf})/2K_{bf})} \quad (7)$$

here, r_{bf} and r_{CNT} are the radius of water molecular ($\approx$0.1 nm) and MWCNTs ($\approx$10 nm). n is the empirical shape factor for MWCNTs calculated from MWCNT parameters to be 14.

The results estimated from the models are shown in Fig. 8. Maxwell model was proved to be inadequate, the calculated data is much lower than the experimental data. This is due to this model only includes the effects of CNT concentration, the thermal conductivity of CNTs and base fluid and do not take into account the effect of CNT size and the thermal interface resistance between the CNTs and base fluid. Moreover, this model seems to more suitable to be applied for spherical particles.[70] In the H–C model, this model is also not very good for predicting even taken into consideration the effects of CNT size through the empirical shape factor, the calculated results are always higher than the experimental results. In similar, the theoretical predictions still higher than the experimental results observed with Patel *et al.* and Xue model. In several reports, the authors also almost concluded that the calculated value obtained from H–C model always increases greatly with the K_{nf}/K_{bf} increasing when it below 10.[71] Similar to Xue model, the calculated results from Thang *et al.* model seem to predict the thermal conductivity enhancement trends of nanofluids. The results obtained from Thang *et al.* model showed the best correlation in comparison with other models. This could be due

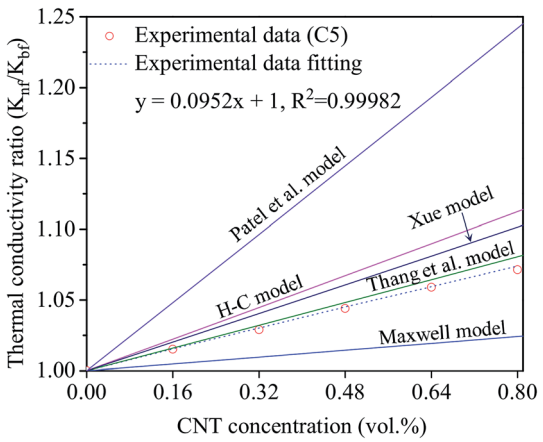

Fig. 8 Comparison of experimental results with serval theoretical models for nanofluid C5.

to Thang's model taken into consideration the effects of size, volume fraction, and thermal conductivity of CNTs as well as the properties of the base liquid. But, noting that the error between the calculated and experimental data seems become clearly as increasing the CNT contents. In fact, Thang *et al.* model also confirmed that their model only validates for nanofluids with the CNT content below 1 vol%.[67] There are many factors lead to the erroneous results calculated by the mentioned models such as the effect of Brown motion, the thermal conductivity of interfacial layer (K_i), type of CNTs, *etc.* In which, the effect of K_i between CNTs and base fluid on the thermal conductivity of CNT based nanofluids is well-known, but K_i was not taken into account for the calculation. This may due to K_i is not exactly known parameter and hardly to be measured by the experiments. Murshed and coworkers have proposed a new model that considered and taken into account the effects of particle size, concentration, and interfacial layer for the calculation.[72,73]

$$K_{nf} = \frac{(K_{CNT} - K_i)\phi K_i(\gamma_1{}^2 - y^2 + 1) + (K_{CNT} + K_i)\gamma_1{}^2[\phi y^2(K_i - K_{bf}) + K_{bf}]}{\gamma_1{}^2(K_{CNT} + K_i) - (K_{CNT} - K_i)\phi(\gamma_1{}^2 + y^2 - 1)} \quad (8)$$

where $\gamma_1 = 1 + t/d_{CNT}$ and $\gamma = 1 + t/r_{CNT}$, and t is the thickness of the interfacial layer between MWCNT and base fluid. As reported by Murshed and coworker, t is estimated to be about 2 nm.[72] The exact value of K_i not known and thus was estimated to be 3 times of the base fluid thermal conductivity. However, the proposed K_i value may not be correct for all cases due to depending on the structure and type of CNTs. So, we used Murshed *et al.* model and the experimental data to estimate and thus clarify the effect of chemical treatment time on the K_i between CNTs and base fluid.

By using Murshed *et al.* model and the experimental data (Fig. 9), K_i values were found to be 1.9 W m^{-1} K^{-1}, 2.6 W m^{-1} K^{-1} and 2.2 W m^{-1} K^{-1} corresponding to nanofluid C3, C5 and C7, respectively. The obtained values are about 3–4 times higher than that of base fluid (0.6 W m^{-1} K^{-1}). This is good agreement with the value proposed by Murshed *et al.*[72] Similar to TBC, the decrease in K_i of nanofluid C3 is attributed to the weak bonding between MWCNTs and base fluid. As for nanofluid C7, the reduction of K_i mainly due to the increase of the defect and disorder points at outside walls of MWCNT resulted from the long chemical treatment time. As results, it is evident here that the thermal conductivity of CNT based nanofluids could be improved by increasing the K_i between CNTs and base fluids. This could be done by either optimizing the chemical treatment condition or employing the suitable surfactants.

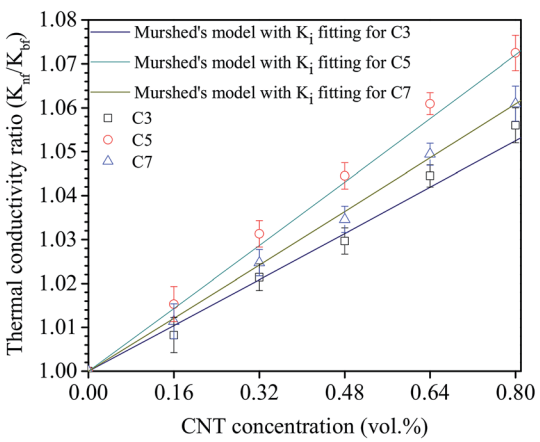

Fig. 9 The thermal conductivity predicted by Murshed *et al.* model with K_i fitting for nanofluids.

4. Conclusions

The influence of chemical treatment time on the structure of MWCNT–COOH and their nanofluids were investigated. The structural defects of MWCNT–COOH increase with increasing the treatment time. Nanofluids showed better stability with more prolonged treatment time due to increasing of COOH functional groups attached to the surface of MWCNTs with increasing the treatment time. The electrical conductivity of the nanofluids containing MWCNT–COOH increases with increasing CNT concentrations and decrease with increasing the chemical treatment time. The nanofluids showed the thermal conductivity improvement when increasing the CNT concentrations and reached to highest value for nanofluid containing MWCNT–COOH with 5 h chemical treatment. By using the EMT and experimental data fitting, the TBR and the TBC of MWCNT–COOH/water were determined to be 90 × 10^{-8} m^2 K W^{-1} and 1.1 MW m^{-2} K^{-1}, respectively. The K_i between CNTs and base fluid was also estimated by using Murshed *et al.* model. The highest K_i was obtained to be 2.6 W m^{-1} K^{-1} for nanofluid C5, implying that the thermal conductivity of CNT based nanofluids could be improved by increasing the K_i *via* optimizing of the chemical treatment condition.

Conflicts of interest

There are no conflicts to declare.

Acknowledgements

The research was financially supported by the National Foundation for Science and Technology Development (NAFOSTED) under a project 103.99-2015.70. This work is also supported by Vietnam Academy of Science and Technology under project No. VAST.TĐ.QP.03/17-19 and VAST.03.02/16-17.

References

1 Q. Zhang, J. Q. Huang, W. Z. Qian, Y. Y. Zhang and F. Wei, *Small*, 2013, **9**, 1237–1265.

2 W. W. Liu, S. P. Chai, A. R. Mohamed and U. Hashim, *J. Ind. Eng. Chem.*, 2014, **20**, 1171–1185.
3 S. B. Sinnott and R. Andrews, *Crit. Rev. Solid State Mater. Sci.*, 2001, **26**, 145–249.
4 M. N. Afiq, W. M. Yazid, N. A. C. Sidik and W. J. Yahya, *Renewable Sustainable Energy Rev.*, 2017, **80**, 914–941.
5 S. M. S. Murshed and C. A. N. Castro, *Renewable Sustainable Energy Rev.*, 2014, **37**, 155–167.
6 H. Xie and L. Chen, *J. Chem. Eng. Data*, 2011, **56**, 1030–1041.
7 S. A. Angayarkanni and J. Philip, *Adv. Colloid Interface Sci.*, 2015, **225**, 146–176.
8 N. A. C. Sidik, M. N. A. W. M. Yazid and S. Samion, *Int. J. Heat Mass Transfer*, 2017, **111**, 782–794.
9 P. Estellé, O. Mahian, T. Maré and H. F. Öztop, *J. Therm. Anal. Calorim.*, 2017, **128**, 1765–1770.
10 S. M. S. Murshed and C. A. N. de Castro, *Renewable Sustainable Energy Rev.*, 2017, **78**, 821–833.
11 S. M. S. Murshed and P. Estellé, *Renewable Sustainable Energy Rev.*, 2017, **76**, 1134–1152.
12 S. Mallakpour and S. Soltanian, *RSC Adv.*, 2016, **6**, 109916–109935.
13 K. Balasubramanian and M. Burghard, *Small*, 2005, **1**, 180–192.
14 T. X. Phuoc, M. Massoudi and R. H. Chen, *Int. J. Therm. Sci.*, 2011, **50**, 12–18.
15 Y. Ding, H. Alias, D. Wen and R. A. Williams, *Int. J. Therm. Sci.*, 2006, **49**, 240–250.
16 A. D. Manasrah, T. Laoui, S. J. Zaidi and M. A. Atieh, *Exp. Therm. Fluid Sci.*, 2017, **84**, 231–241.
17 S. Harish, K. Ishikawa, E. Einarsson, S. Aikawa, *et al.*, *Mater. Express*, 2012, **2**, 213–223.
18 S. Harish, K. Ishikawa, E. Einarsson, S. Aikawa, *et al.*, *Int. J. Heat Mass Transfer*, 2012, **55**, 3885–3890.
19 Y. Xing, L. Li, C. C. Chusuei and R. V. Hull, *Langmuir*, 2005, **21**, 4185–4190.
20 A. G. Osorio, I. C. L. Silveira, V. L. Bueno and C. P. Bergmann, *Appl. Surf. Sci.*, 2005, **255**, 2485–2489.
21 M. N. Tchoul, W. T. Ford, G. Lolli, D. E. Resasco and S. Arepalli, *J. Mater. Chem.*, 2007, **19**, 5765–5772.
22 J. A. R. Babu, K. K. Kumar and S. S. Rao, *Renewable Sustainable Energy Rev.*, 2017, **77**, 551–565.
23 K. Y. Leong, K. Z. K. Ahmad, H. C. Ong, M. J. Ghazali and A. Baharum, *Renewable Sustainable Energy Rev.*, 2017, **75**, 868–878.
24 N. A. C. Sidik, M. M. Jamil, W. M. A. A. Japar and I. M. Adamu, *Renewable Sustainable Energy Rev.*, 2017, **80**, 1112–1122.
25 S. M. G. Babita and S. K. Sharma, *Exp. Therm. Fluid Sci.*, 2016, **79**, 202–212.
26 M. E. Meibodi, M. Vafaie-Sefti, A. M. Rashidi, A. Amrollahi, M. Tabasi and H. S. Kalal, *Int. Commun. Heat Mass Transfer*, 2010, **37**, 319–323.
27 Y. Hwang, Y. Ahn, H. Shin, C. Lee, G. Kim, H. Park and J. Lee, *Curr. Appl. Phys.*, 2006, **6**, 1068–1071.
28 Y. Hwang, J. K. Lee, C. H. Lee, Y. M. Jung, S. I. Cheong, C. G. Lee, B. C. Ku and S. P. Jang, *Thermochim. Acta*, 2007, **455**, 70–74.
29 H. Xie, H. Lee, W. Youn and M. Cho, *J. Appl. Phys.*, 2003, **94**, 4967.
30 J. Koo, Y. Kang and C. Kleinstreuer, *Nanotechnology*, 2008, **19**, 375705.
31 P. Estellé, S. Halelfadl and T. Maré, *Int. Commun. Heat Mass Transfer*, 2014, **57**, 8–12.
32 A. Nasiri, M. Shariaty-Niasar, A. M. Rashidi and R. Khodafarin, *Int. J. Heat Mass Transfer*, 2012, **55**, 1529–1535.
33 A. Ghozatloo, A. M. Rashidi and M. Shariaty-Niasar, *Int. Commun. Heat Mass Transfer*, 2014, **54**, 1–7.
34 J. Glory, M. Bonetti, M. Helezen, M. Mayne-L'Hermite and C. Reynaud, *J. Appl. Phys.*, 2008, **103**, 094309.
35 P. Ganesh Kumar, V. Kumaresan and R. Velraj, *Fullerenes, Nanotubes, Carbon Nanostruct.*, 2017, **25**, 230–240.
36 A. Al-Sharafi, A. Z. Sahin and B. S. Yilbas, *J. Heat Transfer*, 2016, **138**, 072401.
37 N. D. Dung, N. V. Chuc, N. T. T. Tam, N. H. Quang, P. H. Khoi and P. N. Minh, *J. Korean Phys. Soc.*, 2008, **52**, 1372–1377.
38 J. Jang, J. Bae and S. Yoon, *J. Mater. Chem.*, 2003, **13**, 676–681.
39 P. V. Trinh, N. N. Anh, B. H. Thang, L. D. Quang, *et al.*, *RSC Adv.*, 2017, **7**, 318–326.
40 S. Sweeney, S. Hu, P. Ruenraroengsak, S. Chen, A. Gow, *et al.*, *Environ. Sci.: Nano*, 2016, **3**, 1340–1350.
41 M. Khazaee, W. Xia, G. Lackner, R. G. Mendes, M. Rümmeli, M. Muhler and D. C. Lupascu, *Sci. Rep.*, 2016, **6**, 26208.
42 K. Zhang and Q. Zhang, *J. Phys. Chem. C*, 2015, **119**, 18753–18761.
43 S. L. H. Rebelo, A. Guedes, M. E. Szefczyk, A. M. Pereir, J. P. Araújo and C. Freire, *Phys. Chem. Chem. Phys.*, 2016, **18**, 12784–12796.
44 S. Habibzadeh, A. K. Beydokhti, A. A. Khodadadi, Y. Mortazavi, S. Omanovic and M. S. Niassar, *Chem. Eng. J.*, 2010, **156**, 471–478.
45 A. Ghadimi, R. Saidur and H. S. C. Metselaar, *Int. J. Heat Mass Transfer*, 2011, **54**, 4051–4068.
46 J. Ivall, G. Langlois-Rahme, S. Coulombe and P. Servio, *Nanotechnology*, 2017, **28**, 055702.
47 J. O. Aguilar, J. R. Bautista-Quijano and F. Avilés, *eXPRESS Polym. Lett.*, 2010, **4**, 292–299.
48 A. M. Marconnet, M. A. Panzer and K. E. Goodson, *Rev. Mod. Phys.*, 2013, **85**, 1296–1327.
49 M. O. McLinden, S. A. Klein, E. W. Lemmon and A. P. Peskin, *NIST Thermodynamic and Transport Properties of Refrigerant Mixtures—REFPROP, Version 6.01, NIST Standard Reference Database 23*, National Institute of Standards and Technology, Gaithersburg, MD, 1998.
50 M. J. Assael, I. N. Metaxa, K. Kakosimos and D. Constantinou, *Int. J. Thermophys.*, 2006, **27**, 999–1016.
51 L. Chen, H. Xie, Y. Li and W. Yu, *Thermochim. Acta*, 2008, **477**, 21–24.
52 A. Amrollahi, A. A. Hamidi and A. M. Rashidi, *Nanotechnology*, 2008, **19**, 315701.
53 M. S. Liu, M. C. C. Lin, I. T. Huang and C. C. Wang, *Int. Commun. Heat Mass Transfer*, 2005, **32**, 1202–1210.

54 B. Munkhbayar, M. Bat-Erdene, B. Ochirkhuyag, D. Sarangerel, B. Battsengel, H. Chung and H. Jeong, *Mater. Res. Bull.*, 2012, **47**, 4187–4196.
55 H. Xie and L. Chen, *Phys. Lett. A*, 2009, **373**, 1861–1864.
56 S. S. J. Aravind, P. Baskar, T. T. Baby, R. K. Sabareesh, S. Das and S. Ramaprabhu, *J. Phys. Chem. C*, 2011, **115**, 16737–16744.
57 T. T. Baby and R. Sundara, *J. Mater. Chem.*, 2011, **21**, 9702–9709.
58 C. W. Nan, R. Birringer, D. R. Clarke and H. Gleiter, *J. Appl. Phys.*, 1997, **81**, 6692–6699.
59 A. Balandin, *Nat. Mater.*, 2011, **10**, 569–581.
60 Z. G. Fthenakis, Z. Zhu and D. Tomanek, *Phys. Rev. B: Condens. Matter Mater. Phys.*, 2014, **89**, 125421.
61 E. Chiavazzo and P. Asinari, *Nanoscale Res. Lett.*, 2011, **6**, 249.
62 S. Hida, T. Hori, T. Shiga, J. Elliott and J. Shiomi, *Int. J. Heat Mass Transfer*, 2013, **67**, 1024–1029.
63 S. T. Huxtable, D. G. Cahill, S. Shenogin, L. Xue, R. Ozisik, P. Barone, *et al.*, *Nat. Mater.*, 2003, **2**, 731–734.
64 C. F. Carlborg, *Phys. Rev. B: Condens. Matter Mater. Phys.*, 2008, **78**, 1–8.
65 J. C. Maxwell, *A Treatise on Electricity and Magnetism*, UK, Clarendon, 1973.
66 R. L. Hamilton and O. K. Crosser, *Ind. Eng. Chem. Fundam.*, 1962, **1**, 187–191.
67 B. H. Thang, P. H. Khoi and P. N. Minh, *Phys. Fluids*, 2015, **27**, 032002.
68 H. E. Patel, K. B. Anoop, T. Sundararajan and S. K. Das, *Bull. Mater. Sci.*, 2008, **31**, 387–390.
69 Q. Z. Xue, *Phys. B*, 2005, **368**, 302–307.
70 P. M. Kumar, J. Kumar, R. Tamilarasan, S. Sendhilnathan and S. Suresh, *Eng. J.*, 2015, **19**, 67–83.
71 L. Yang and X. Xu, *Int. Commun. Heat Mass Transfer*, 2017, **81**, 42–50.
72 S. M. S. Murshed, K. C. Leong and C. Yang, *Int. J. Therm. Sci.*, 2008, **47**, 560–568.
73 P. Estellé, S. Halelfadl and T. Mare, *J. Therm. Eng.*, 2015, **1**, 381–390.